Real-Time Digital Fringe Projection Measurement for Detecting Back Shape in Scoliosis

Hung-Ju Chung, Shuo-Chih Chien, Ching-Hua Lu, and Cheng-Yang Liu
Department of Biomedical Engineering, National Yang Ming Chiao Tung University, Taipei City, Taiwan
Email: cyliu66@ym.edu.tw

***Abstract*—The purpose of this study is to develop low-cost real-time digital fringe projection measurement to detect the three-dimensional shape of the back in patients with scoliosis. The measurement system consists of a digital projector and a digital camera. The seven fringe patterns are used to illuminate a patient's back while the digital images are captured by a camera. The height of the back shape is calculated using the seven-step phase-shifting calculation and path-independent phase unwrapping. The back topography with an accuracy of 1 mm can help the clinician to estimate the spinal deformity at baseline and monitor variations over time. The measurement results can be applied to clinical use and reduce the dependence on serial radiography for monitoring spinal deformity.**

***Index Terms*—fringe projection, phase shifting, scoliosis**

I. Introduction

Scoliosis is a sideways deformity of the spine in Three-Dimensional (3-D) space, which often occurs in adolescents. It can be observed from the asymmetry between two shoulders, an abnormal uplift of thoracic or lumbar [1], [2]. While most cases of scoliosis are mild, severe scoliosis can cause damage to the development period. Traditionally, scoliosis is monitored with radiography, but patients will accumulate large doses of radiation throughout years of treatment [3], [4]. Nowadays, multiple radiation-free, contactless 3-D shape measurements are developed. But advanced methods used on scoliosis patients such as laser ultrasound and inertial sensors require operators to have certain techniques, and the required devices cannot be obtained easily [5]-[8]. Meanwhile, digital phase-shifting fringe projection profilometry has been used for various purposes in consideration of its advantages such as easy implementation, low cost, high accuracy, and real-time dense point cloud capturing [9]-[13]. The fundamental mechanism of this method is to find homologous points from captured images, calculate the deformation of the object, and extract the shape information into phase values. Before putting the system into use, the camera needs to be calibrated by acquiring its intrinsic and extrinsic parameters, which is required to calculate the error between the camera system and the actual image. Radial and tangential distortion caused by the lens is also considered during the calibration process. The nonlinearity of grey values in an image can cause error in computing phase value. Therefore, gamma decoding fringe is introduced to make sure that the camera responses to different light intensities in a linear pattern. In this study, we propose low-cost real-time digital fringe projection measurement to detect the 3-D shape of the back in patients with scoliosis. The measurement results can help the clinician to estimate the spinal deformity at baseline.

Manuscript received May 18, 2021; revised August 12, 2021.

II. Principle of Measurement

Digital fringe projection measurement system is used for high-speed detecting the 3-D shape of human back. Fig. 1(a) shows the measurement system composed of a digital projector, a camera with a resolution of 1920×1080 and an industrial computer. The projector casts seven fringe patterns consecutively on the human back and each time creates different deformed patterns on the back surface. Fig. 1(c) shows the deformed fringe pattern on the human back. The deformed phase-shifted fringe patterns are used to reconstruct the 3-D shape of human back through phase wrapping, phase unwrapping calculations and phase to dimension conversion.

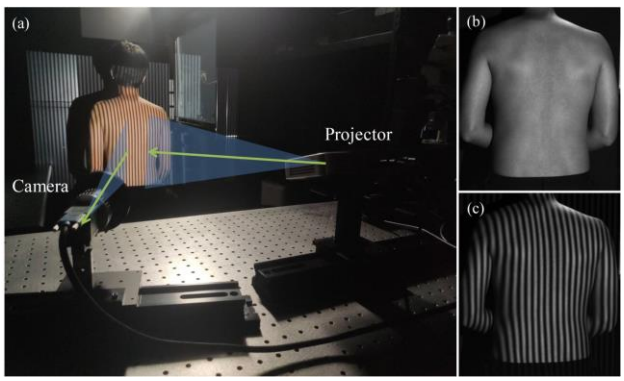

Figure 1. (a) Digital fringe projection measurement system. Images of human back (b) without and with (c) fringe patterns.

The seven-step phase-shifting calculation is suitable for high-resolution 3-D measurement. To reach adequate images for seven-step processing, there is a $\pi/2$ gap

doi: 10.18178/ijeee.9.3.65-69

between each fringe pattern, which can be described mathematically:

$$
\begin{aligned}
I_1(i,j) &= I_B(i,j) + I_A(i,j)\cos[\phi(i,j) - \frac{3\pi}{2}] \\
I_2(i,j) &= I_B(i,j) + I_A(i,j)\cos[\phi(i,j) - \pi] \\
I_3(i,j) &= I_B(i,j) + I_A(i,j)\cos[\phi(i,j) - \frac{\pi}{2}] \\
I_4(i,j) &= I_B(i,j) + I_A(i,j)\cos[\phi(i,j)] \\
I_5(i,j) &= I_B(i,j) + I_A(i,j)\cos[\phi(i,j) + \frac{\pi}{2}] \\
I_6(i,j) &= I_B(i,j) + I_A(i,j)\cos[\phi(i,j) + \pi] \\
I_7(i,j) &= I_B(i,j) + I_A(i,j)\cos[\phi(i,j) + \frac{3\pi}{2}]
\end{aligned}
\quad (1)
$$

In Eq. (1), I_n is the intensity distribution of the n-th pattern for each step. I_B represents the background light intensity of the surroundings. *IA* means the light intensity of the amplitude of each cosine fringe pattern. The industrial computer receives the images captured by the digital camera, and uses the following equation to transform it into phase data:

$$
\phi(i,j) = \tan^{-1}\left(\frac{3I_3(i,j) + I_7(i,j) - I_1(i,j) - 3I_5(i,j)}{4I_4(i,j) - 2I_2(i,j) - 2I_6(i,j)}\right) \quad (2)
$$

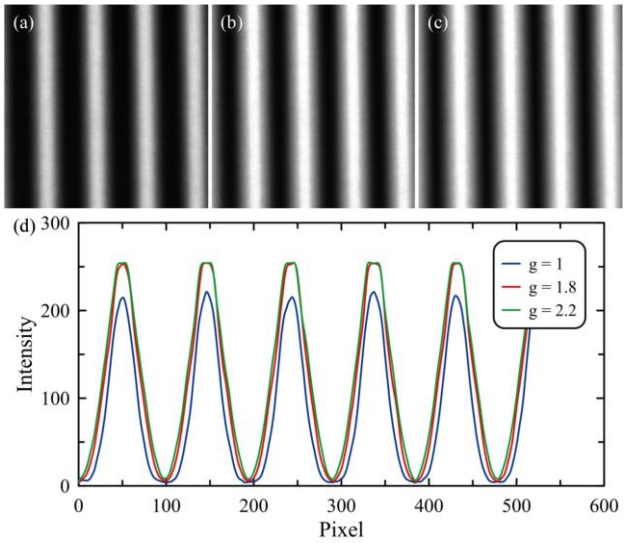

Figure 2. Fringe patterns at gamma value (a) g = 1, (b) g = 1.8, and (c) g = 2.2. (d) Intensity profiles of the fringe patterns at different gamma values.

ψ(*i*, *j*) in Eq. (2) indicates the phase value in every pixel of the cosine fringe pattern. In order to undo the gamma correction of the camera, a gamma decoding fringe is projected on the object surface. Fig. 2(a) to Fig. 2(c) show the fringe patterns at different gamma values. To determine the gamma value (g) for fringe correction, a simple test by casting a large grayscale on a white sheet is performed. Fig. 2(d) shows the intensity profiles of the fringe patterns at different gamma values. The blue line is the intensity profile when the camera receives data from the fringe pattern at g = 1, red line is the intensity profile at g = 1.8, and green line is the intensity profile at g = 2.2. The results show that when the gamma decoding fringe is at g = 1.8, the camera responses the most linearly among others. On the other hand, lens distortion is corrected by the calibration algorithm using pre-acquired parameters. The continuous phase values are obtained by phase unwrapping calculation. Because the quality guided path calculation is suitable for unwrapping complex phase map, we use quality guided path algorithm for unwrapping calculation in this study.

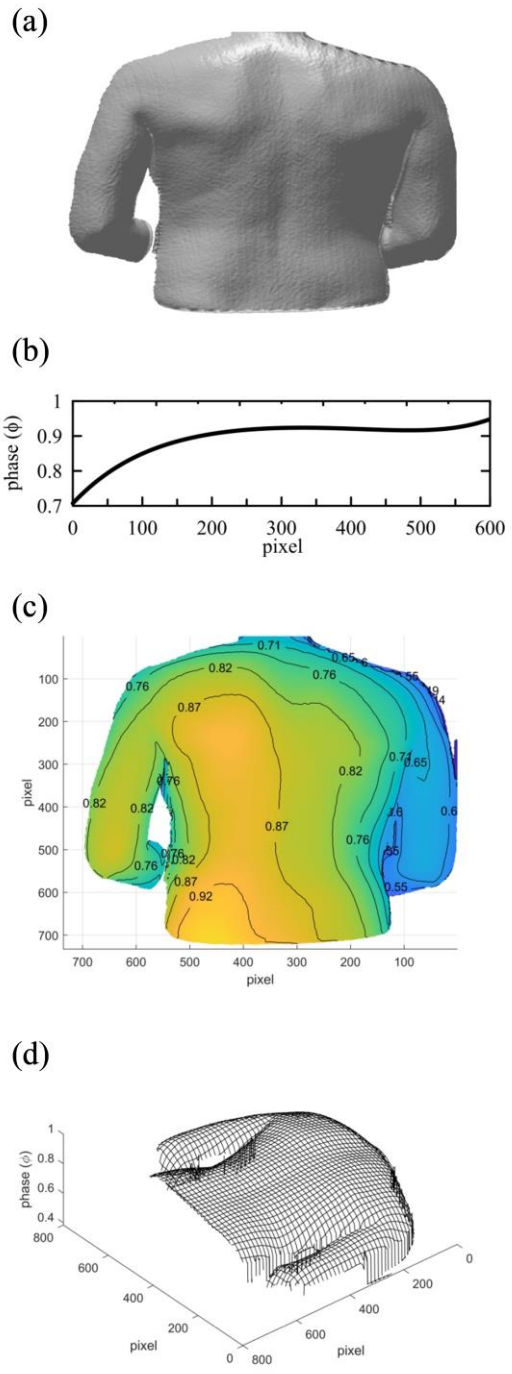

Figure 3. 3-D representations of human back: (a) 3-D model, (b) back profile along the middle line of the spine, (c) contour map, and (d) height map.

III. Results and Discussion

The deformed fringe patterns are used to reconstruct the 3-D model of human back through phase wrapping, phase unwrapping and phase to real size conversion. Fig. 3 shows the 3-D representations of the captured human back. The experimental results clearly show that the fringe projection technique correctly obtains the 3-D surface of human back. The seven-step phase-shifting computation obviously mended the smoothness of the back surface, as shown in Fig. 3(a). The nonlinear phase errors in the 3-D model are balanced by quality guided path unwrapping. The measurement capabilities of large-area and high-resolution for human back are well proven. In Fig. 3(b), the back profile along the middle line of the spine is provided by slicing the 3-D model and allows fast identification for kyphosis and lordosis. Fig. 3(c) and Fig. 3(d) show the contour and height maps, which are useful for giving a quick overview of the back. The small dents or bulges in the back can be identified by the contour maps that are often hard to distinguish with the naked eye.

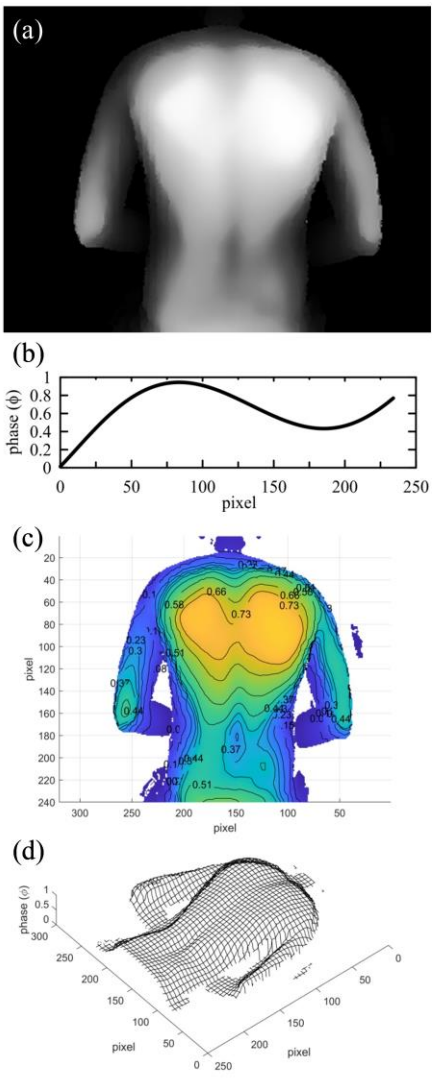

Figure 4. 3-D depth images of human back: (a) 3-D view, (b) back profile along the middle line of the spine, (c) contour map, and (d) height map.

The experimental results are compared with 3-D depth images by using a depth camera (Intel RealSense SR305). The depth camera also uses coded light technique for scanning and reconstruction. The experimental target and environment are maintained for comparison. Fig. 4(a) shows the 3-D depth image of human back. The height variation of human back can be observed by the bright region of depth image. In Fig. 4(b), the curvature of the spine can be distinctively identified by using the back profile. The height and contour maps locate the positions of the subscapular bones and other landmarks for measurement. However, the height information will be enhanced in the depth images and the 3-D shape of the whole human back will be distorted.

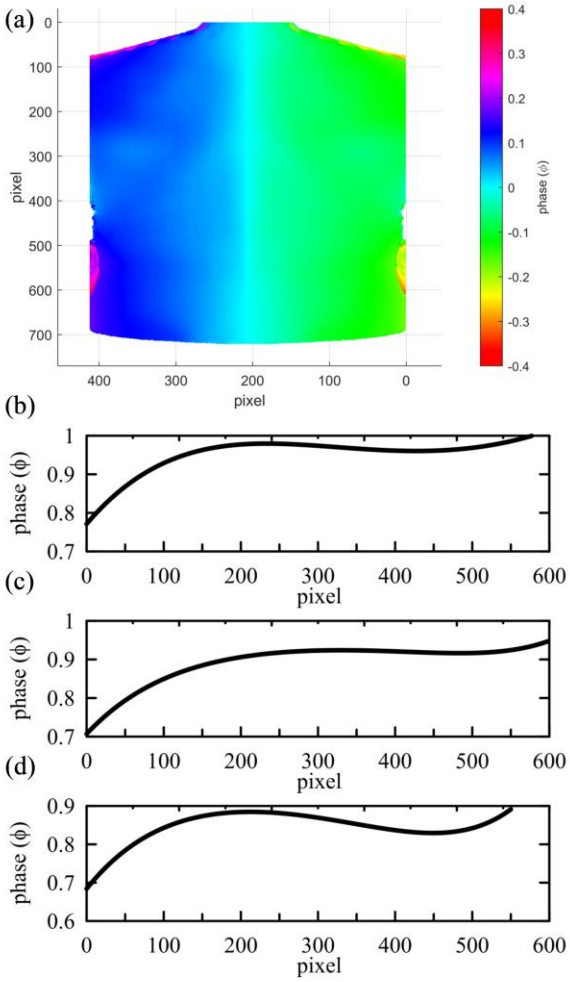

Figure 5. (a) Bilateral asymmetry map of human back. Back profiles along the (b) right subscapular bone, (c) middle line of the spine, and (d) left subscapular bone.

The measured 3-D model by this experiment is further processed into bilateral asymmetry map. The bilateral asymmetry map is useful for determining the balance of two sides of the human back. It can clearly be seen in Fig. 5(a) that the left side of the human back is higher than the right side. Fig. 5(b) to Fig. 5(d) show the back profiles along the right subscapular bone, middle line of the spine, and left subscapular bone. These back profiles can be used to inspect the curvature of the back in different angles.

IV. Conclusion

In this study, a high-speed digital fringe projection technique is proposed to measure the 3-D model of human back. A digital projector is used as the light source to project several fringe patterns onto the back surface. The gamma decoding fringes are introduced for gamma correction and higher accuracy. The distorted fringe images from the back surface are captured by the digital camera. The phase data in the distorted fringe images are obtained by using the seven-step phase-shifting and quality guided path unwrapping calculations. The image acquisition, reconstruction and exhibition of the 3-D back model have performed simultaneously at a speed of 1 second. Post processing of the 3-D back model such as contour and height maps gives more information for further utilization. This experiment proposes a real-time 3-D measurement which is capable of scanning large objects in high resolution.

Conflict of Interest

The authors declare no conflict of interest.

Author Contributions

Hung-Ju Chung, Shuo-Chih Chien, and Ching-Hua Lu conducted the research; Shuo-Chih Chien and Cheng-Yang Liu analyzed the data and wrote the paper; all authors had approved the final version.

Acknowledgment

The authors would like to appreciate the partial financial support from the Ministry of Science and Technology in Taiwan with the project number of MOST 108-2221-E-010-012-MY3 and MOST 109-2923-E-010-001-MY2.

References

[1] M. Konieczny, H. Senyurt, and R. Krauspe, "Epidemiology of adolescent idiopathic scoliosis," *Journal of Children's Orthopaedics*, vol. 7, pp. 3-9, 2013.

[2] A. Gardner, F. Berryman, and P. Pynsent, "A description of three-dimensional shape of the posterior torso comparing those with and without scoliosis," *Symmetry*, vol. 11, p. 211, 2019.

[3] S. Himmetoglu, M. Guven, N. Bilsel, and Y. Dincer, "DNA damage in children with scoliosis following X-ray exposure," *Minerva Pediatr.*, vol. 67, pp. 245-249, 2015.

[4] F. Berryman, P. Pynsent, J. Fairbank, and S. Disney, "A new system for measuring three-dimensional back shape in scoliosis," *European Spine Journal*, vol. 17, pp. 663-672, 2008.

[5] V. Zarubin, A. Bychkov, A. Karabutov, V. Simonova, I. Kudinov, and E. Cherepetskaya, "Real-time laser ultrasound tomography for profilometry of solids," *Moscow University Physics Bulletin*, vol. 73, pp. 75-82, 2018.

[6] S. Park, S. Baik, H. Cha, Y. Cheong, W. Kim, C. Cho, and Y. Kang, "Laser ultrasonic inspection system with a 3d surface profilometry to detect surface cracks," *Modern Physics Letters B*, vol. 22, pp. 1051-1056, 2008.

[7] V. Zarubin, A. Bychkov, A. Karabutov, V. Simonova, and E. Cherepetskaya, "A method of laser ultrasound tomography for solid surfaces mapping," *MATEC Web of Conferences*, vol. 145, p. 05009, 2018.

[8] A. Fathi, and K. Curran, "Detection of spine curvature using wireless sensors," *Journal of King Saud University-Science*, vol. 29, pp. 553-560, 2017.

[9] C. Liu and T. Yen, "Digital multi-step phase-shifting profilometry for three-dimensional ballscrew surface imaging," *Optics & Laser Technology*, vol. 79, pp. 115-123, 2016.

[10] A. Babaei, M. Saadatseresht, and J. Kofman, "Exponential fringe pattern projection approach to gamma-independent phase computation without calibration for gamma nonlinearity in 3D optical metrology," *Optics Express*, vol. 25, pp. 24927-24938, 2017.

[11] Y. Hu, Q. Chen, Y. Zhang, S. Feng, T. Tao, H. Li, W. Yin, and C. Zuo, "Dynamic microscopic 3D shape measurement based on marker-embedded Fourier transform profilometry," *Applied Optics*, vol. 57, pp. 772-780, 2018.

[12] C. Jiang, B. Lim, and S. Zhang, "Three-Dimensional shape measurement using a structured light system with dual projectors," *Applied Optics.*, vol. 57, pp. 3983-3990, 2018.

[13] C. Lin, Z. Qiu, and C. Yeh, "Image processing for rear foot image evaluating leg and foot angles," *Measurement*, vol. 126, pp. 168-183, 2018.

[14] B. Li, and S. Zhang, "Novel method for measuring a dense 3D strain map of robotic flapping wings," *Measurement Science and Technology*, vol. 29, pp. 045402, 2018.

[15] Y. Arieli, S. Epshtein, A. Harris, I. Yaacubov, and Y. Cohen, "Full field tomography using interference fringes casting of a non spatially-coherent extended spectrally modulated broadband light source," *Optics Communications*, vol. 407, pp. 426-431, 2018.

[16] C. Chen, N. Gao, X. Wang, and Z. Zhang, "Adaptive projection intensity adjustment for avoiding saturation in three-dimensional shape measurement," *Optics Communications*, vol. 410, pp. 694-702, 2018.

[17] S. Yu, J. Zhang, X. Yu, X. Sun, H. Wu, and X. Liu, "3D measurement using combined Gray code and dual-frequency phase-shifting approach," *Optics Communications*, vol. 413, pp. 283-290, 2018.

[18] J. Flores, G. Ayubi, J. Martino, O. Castillo, and J. Ferrari, "3D-shape of objects with straight line-motion by simultaneous projection of color coded patterns," *Optics Communications*, vol. 414, pp. 185-190, 2018.

[19] J. Hyun, G. Chiu, and S. Zhang, "High-speed and high-accuracy 3D surface measurement using a mechanical projector," *Optics Express*, vol. 26, pp. 1474-1487, 2018.

[20] H. Zhao, Y. Xu, H. Jiang, and X. Li, "3D shape measurement in the presence of strong interreflections by epipolar imaging and regional fringe projection," *Optics Express*, vol. 26, pp. 7117-7131, 2018.

[21] Z. Liu, P. Zibley, and S. Zhang, "Motion-induced error compensation for phase shifting profilometry," *Optics Express*, vol. 26, pp. 12632-12637, 2018.

[22] G. Rao, L. Song, S. Zhang, X. Yang, K. Chen, and J. Xu, "Depth-driven variable-frequency sinusoidal fringe pattern for accuracy improvement in fringe projection profilometry," *Optics Express*, vol. 26, pp. 19986-20008, 2018.

[23] Y. Wang, Z. Liu, C. Jiang, and S. Zhang, "Motion induced phase error reduction using a Hilbert transform," *Optics Express*, vol. 26, pp. 34224-34235, 2018.

[24] C. Zhang, H. Zhao, J. Qiao, C. Zhou, L. Zhang, G. Hu, and H. Geng, "Three-Dimensional measurement based on optimized circular fringe projection technique," *Optics Express*, vol. 27, pp. 2465-2477, 2019.

[25] H. Zhang, H. Zhao, Z. Zhao, Y. Zhuang, and C. Fan, "Two-Frame fringe pattern phase demodulation using Gram-Schmidt orthonormalization with least squares method," *Optics Express*, vol. 27, pp. 10495-10508, 2019.

[26] Y. Xu, H. Zhao, H. Jiang, and X. Li, "High-Accuracy 3D shape measurement of translucent objects by fringe projection profilometry," *Optics Express*, vol. 27, pp. 18421-18434, 2019.

[27] P. Zhou, J. Zhu, and Z. You, "3-D face registration solution with speckle encoding based spatial-temporal logical correlation algorithm," *Optics Express*, vol. 27, pp. 21004-21019, 2019.

[28] Z. Wu, W. Guo, and Q. Zhang, "High-Speed three-dimensional shape measurement based on shifting Gray-code light," *Optics Express*, vol. 27, pp. 22631-22644, 2019.

[29] J. Shi, X. Zhu, H. Wang, L. Song, and Q. Guo, "Label enhanced and patch based deep learning for phase retrieval from single frame fringe pattern in fringe projection 3D measurement," *Optics Express*, vol. 27, pp. 28929-28943, 2019.

[30] S. Xing and H. Guo, "Iterative calibration method for measurement system having lens distortions in fringe projection profilometry," *Optics Express*, vol. 28, pp. 1177-1196, 2020.
[31] M. Zhong, X. Hu, F. Chen, C. Xiao, D. Peng, and S. Zhang, "Autofocusing method for a digital fringe projection system with dual projectors," *Optics Express*, vol. 28, pp. 12609-12620, 2020.
[32] Y. Wan, Y. Cao, X. Liu, T. Tao, and J. Kofman, "High-Frequency color-encoded fringe-projection profilometry based on geometry constraint for large depth range," *Optics Express*, vol. 28, pp. 13043-13058, 2020.
[33] H. Yu, D. Zheng, J. Fu, Y. Zhang, C. Zuo, and J. Han, "Deep learning-based fringe modulation-enhancing method for accurate fringe projection profilometry," *Optics Express*, vol. 28, pp. 21692-21703, 2020.
[34] L. Zhang, Q. Chen, C. Zuo, and S. Feng, "Real-Time high dynamic range 3D measurement using fringe projection," *Optics Express*, vol. 28, pp. 24363-24378, 2020.
[35] C. Liu and C. Wang, "Investigation of phase pattern modulation for digital fringe projection profilometry," *Measurement Science Review*, vol. 20, pp. 43-49, 2020.
[36] C. Liu, T. Yen, and C. Chen, "High-Resolution three-dimensional surface imaging microscope based on digital fringe projection technique," *Measurement Science Review*, vol. 20, pp. 139-144, 2020.

Hung-Ju Chung was born in Taiwan in 1997. He is currently working toward the Master's degree at the National Yang Ming Chiao Tung University, Taiwan. His research interests include fringe projection technique and semiconductor device fabrication.

Shuo-Chih Chien was born in Taiwan in 1999. He is currently working toward the Master's degree at the National Yang Ming Chiao Tung University, Taiwan. His research interests include fringe projection technique and semiconductor device fabrication.

Ching-Hua Lu was born in Taiwan in 1997. He is currently working toward the Master's degree at the National Yang Ming Chiao Tung University, Taiwan. His research interests include fringe projection technique and semiconductor device fabrication.

Cheng-Yang Liu was born in Taiwan in 1977. He received the Ph.D. degree from the National Cheng Kung University, Taiwan, in 2005. He is currently a Professor in Department of Biomedical Engineering, National Yang Ming Chiao Tung University, Taiwan. He has published 68 research articles in optical physics and engineering. His research focuses on photonic crystal, light scattering, fringe projection technique, biophotonics, and photonic nanojet.